Table of Contents

Introduction

Photosynthesis

In plants, the photosynthetic light reactions can in general be presented by the scheme shown in Fig.1. In this scheme one can see how photons trigger a long series of events, from the water-splitting reaction at photosystem II (PSII) to the formation of energy-rich molecules such as NADPH and ATP. The electron-transfer chain, maintained by electron-transfer proteins/cofactors such as plastocyanin (Pc), ends with the formation of NADPH and the gradual buildup of a proton gradient across the thylakoid membrane is used for synthesis of ATP, catalyzed by ATP synthase. O_2 is released to the atmosphere while NADPH and ATP are used in the so-called dark reactions to synthesize carbohydrates from carbon dioxide taken up from the air.

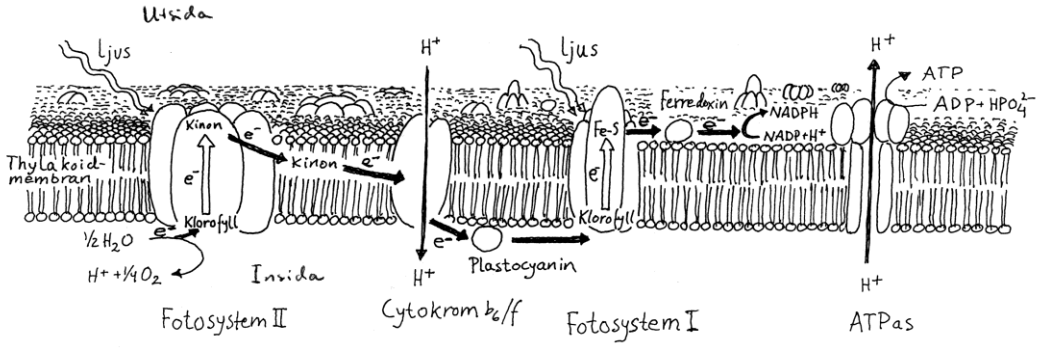

Figure 1: General scheme showing the light reactions in plants and the major components involved. The wonderful illustration in Swedish was borrowed with permission from Lars-Erik Andréasson.

There are two main factors that control the flow of electrons in this electron-transfer chain. First, the redox potential of the electron carriers, second, factors governing the interactions between the electron-carrier proteins. The redox potential attained to drive the oxidation of water (splitting of water molecules) is made possible by the absorption of light and the excitation of the special pair in PS II (Fig. 2). In the excited state, P680* has a significantly lower redox potential and hence is susceptible to oxidation, an electron is transferred. Then, $P680^+$ has a sufficiently high redox potential to oxidize water.

Photosystem I (PSI) is involved in translocating electrons across the thylakoid membrane. Electrons transferred from the electron-carrier protein Pc on the luminal side to ferrodoxin in

the stroma is a result of the driving force generated by the special pair (P700) once photooxidized by sunlight (Fig.2).

The electron donation from Pc to PSI and the regulatory factors that may govern this interaction is the main focus of this thesis.

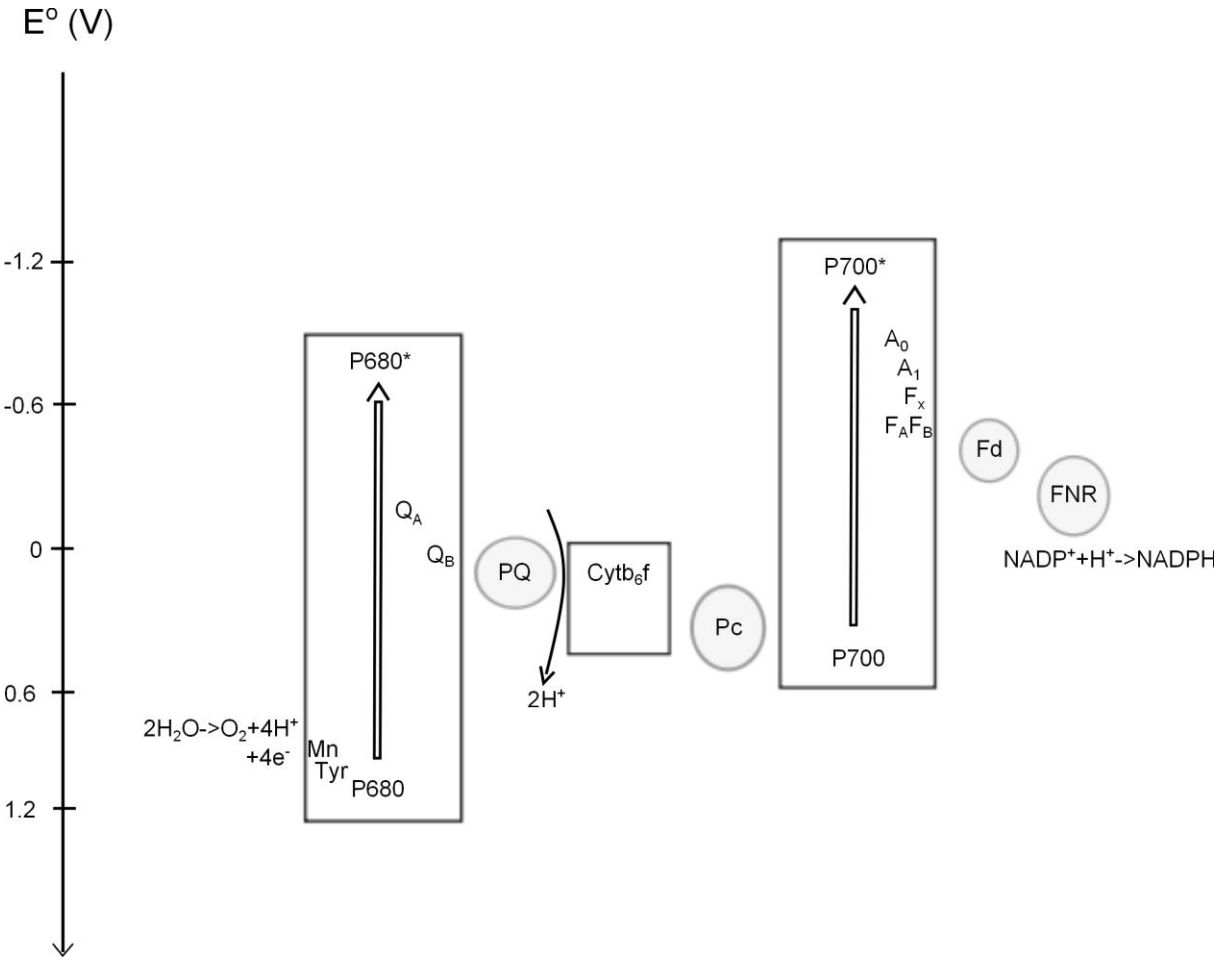

Figure 2: Z-scheme indicating key features of the linear electron-transfer chain in plants. Mobile electron carriers are highlighted in grey. Note that the y-axis has been inverted to emphasize a "down-hill" flow of electrons, from high-energy species to low. * indicates an excited state.

Photosystem I and PsaF

PSI consists of a core complex and a peripheral antenna. In plants, these two functional units are assembled from at least 19 protein subunits. The PSI core complex contains 15 subunits named PsaA to PsaL and PsaN to PsaP, of which many are homologous to their cyanobacterial counterparts [1, 2]. The crystal structure of the PSI super-complex from pea

has been determined to a 3.3 Å resolution and reveals 18 protein subunits, 173 chlorophylls, 2 phylloquinones, 3 Fe_4S_4 clusters and 15 carotenoids [3].

The PSI core subunit explored in the present work, PsaF, is a 17.3 kDa protein that extends through the thylakoid membrane. It consists of both a hydrophobic transmembrane helical region and two hydrophilic regions exposed to either side of the membrane. In plants and algae, the N-terminal region of PsaF, located in the thylakoid lumen, is of particular interest due to its involvement in the binding of Pc [3-9]. ClustalW multiple sequence alignments of the luminal domain of PsaF (Fig. 3) as defined by [3] reveals highly conserved residues Gly4, Leu5, Pro7, Cys8, Lys16, Ala41, Ala44, Arg52, Phe53, Tyr56, Leu61, Leu62, Cys63, Gly64, Gly67, Leu68, Pro69, His70, Leu71, His79, Gly81 and Glu82 of which a large majority are hydrophobic. The numbering of amino acids is with respect to the PsaF sequence from spinach.

```
c    Organism
                          1        10        20        30        40        50
II   |Spinacia           DIAGLTPCKESKQFAKREKQALKKLQASLKLYADDSAPALAIKATMEKTKK
II   |Poplar             DISGLTPCKDSKQFAKREKQQIKKLESSLKLYSPDSAPALAIKATVEKTKR
II   |Barely             DIAGLTPCKESKAFAKREKQSVKKLNSSLKKYAPDSAPALAIQATIDKTKR
II   |Chlamydomonas      DIAGLTPCSESKAYAKLEKKEIKTLEKRLKQYEADSAPAVALKATIERTKT
II   |Micromonas         PYAGLTPCKKNAAFKKREKQEIKALEKRLKKYEEGSAPALALKATQDKTSA
I    |Synechococcus sp. DVAGLVPCNESAAFQKR----------------------AAAAPTDEAKA


                               60        70            80
II   |Spinacia           RFDNYGKYGLLCGSDGLPHLIVSG----DQRHWGEF
II   |Poplar             RFDNYGKQGLLCGSDGLPHLIVSG----DQRHWGEF
II   |Barely             RFENYGKFGLLCGSDGLPHLIVSG----DQRHWGEF
II   |Chlamydomonas      RFANYAKAGLLCGNDGLPHLIADPGLALKYGHAGEV
II   |Micromonas         RFKAYGEAGLLCGADGLPHLIVDG----NLEHLGEF
I    |Synechococcus sp. RFEFYGNTSLLCGPEGLPHLVVDG----DLAHAGEF
```

Figure 3: ClustalW multiple sequence alignment of the N-terminal domain of PsaF, class I: Prokaryote (cyanobacteria) Class II: Eukaryote (green algae and plant).

From the crystal structures of plant [3] and cyanobacterial [10] PsaF, one can note that most of the conserved hydrophobic residues mentioned previously are localized around Cys8 and Cys63 or the corresponding residues in cyanobacteria. The lumen-exposed domain consists of a helix-loop-helix region between the two Cys residues. In green algae and plants the helix-loop-helix region is extended by residues 18-41. The sequence shows low complexity (only a

few different types of amino acids) in the region 19-31 of which many residues are positively charged Lys. Furthermore, the positively charged residues Lys19, Lys23, Lys30 are conserved among all algae and plants. In contrast to cyanobacteria, plant PsaF is known to interact specifically with Pc. In fact, in plants, PsaF is responsible for enhancing the electron donation to PS I by a 100 fold. A residue of significant importance for maintaining an efficient binding of Pc is Lys23 [11].

Interestingly, in cyanobacteria (X-ray crystal structure pdb 1jb0) Cys8 and 43 form a disulphide bond [10]. This is in contrast to the corresponding residues in plants (Cys8 and 63), where the conserved cysteines are in their reduced form [3, 4] (pdb 3lw5, 2o01). The redox state of the cysteines will be addressed in Paper I of this thesis. It will be shown that the luminal domain of PsaF is more stable when they are forming a disulphide bond and then the protein can also cross-link more efficiently to Pc.

Plastocyanin

Pc is a blue copper protein of ~10kDa found in all plants and algae and in many cyanobacteria. In green algae and cyanobacteria, in the presence of copper, Pc may replace the heme-containing functional analogue cytochrome c_6 (Cyt c_6) [12]. In plants, the gene encoding for Cyt c_{6A}, a homologue to Cyt c_6, can be found, however its function is yet unknown. It was recently suggested that Cyt c_{6A} may be involved in thiol-disulphide exchange reactions within the thylakoid lumen [13]. Both *in-vivo* mutagenesis studies (in *Arabidopsis*) and *in-vitro* studies showed that Cyt c_{6A} cannot shuttle electrons between the cytochrome b_6f complex and PSI, hence suggesting that Pc has evolved to replace the function of Cyt c_6 in plants [14, 15].

Comparisons of the primary sequence of Pc show that the copper ligands His37, His87, Cys84 and Met92 are conserved among all Pc-containing organisms. Many hydrophobic residues (Pro, Tyr, Ala and Gly), thought to be important for preserving the tertiary fold and to form a hydrophobic patch surrounding the bound copper, are also conserved. Amongst higher plants and algae, two regions of conserved negatively charged residues (Asp and Glu) can be found. The two regions include residues 42-44 and 59-61 [16, 17] and are usually called the lower and upper acidic patches, respectively.

The first structure of Pc was published in 1978 at a 2.7 Å resolution. The source was poplar and the method by which the structure was solved was X-ray crystallography [18]. Some years later in 1988, the first solution NMR structure was determined for Pc and the source was *Scenedesmus obliquus.* Many additional structures of Pc from a variety of sources have also been published [19-21]. Both X-ray and NMR structural studies show a protein forming an anti-parallel eight-strand beta-barrel. The bound copper is coordinated by His37, Cys84, His87 and Met92 in a distorted tetrahedral geometry. This has also been characterized by EPR (Fig. 5A), the small hyperfine coupling (A_z=64 G) is characteristic of a distorted type 1 copper site. The electronic spectrum of oxidized Pc is characterized by a strong Cu-Cys84 charge-transfer band at 597 nm (Fig. 5B). The relatively high midpoint redox potential ($E^{o'}$~380 mV) has been explained as being due to the strained conformation of the copper-site geometry [22]. Furthermore, using X-ray crystallography, Freeman et al. have showed that the Pc structure is essentially unaffected by the copper-site redox state at pH 7-8, hence, facilitating a high electron-transfer rate due to a low reorganization energy [23].

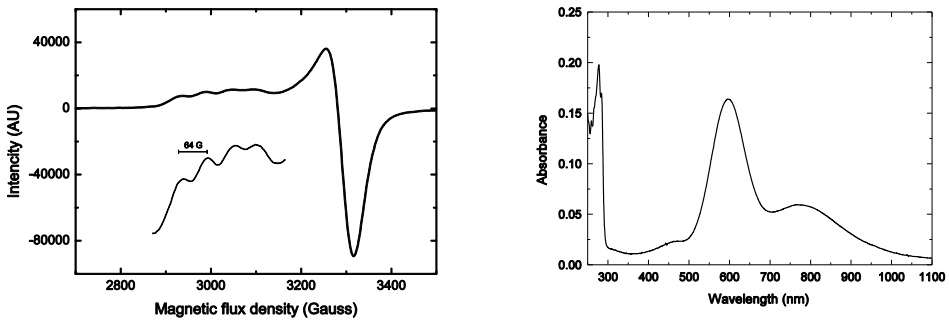

Figure 5: A) X-band EPR spectrum of oxidized Pc at 77 K. B) Electronic absorption spectrum of oxidized Pc.

Studies have revealed two distinct regions on Pc, sites 1 and 2, which are important for the binding and subsequent electron transfer to PSI. The significance of the individual sites varies depending on the organism.

Site 1, the hydrophobic patch, consisting of highly conserved residues Gly10, Leu12 Gly89, Pro36 and Pro86, is located on the northern top of the molecule surrounding His87 of the copper site (Fig. 6). Site 2, the two acidic patches located on the eastern side of Pc (Fig. 6 arrows), includes residues 42-45 and 59-61, with Tyr83 wedged in between the two ridges formed by the two patches. The contribution to the electrostatic field from the two acidic patches gives the molecule a net dipole moment in the corresponding direction [24]. The two

acidic patches can be found in higher plants and green algae, but not in cyanobacteria. The involvement of the two sites in the binding to PSI (and Cyt b_6f) has been explored in several publications and is still a topic of active research. Site 1 has been shown to make specific hydrophobic contacts with lumen-exposed helices of PSI subunits A and B. The conserved Trp residues 651 (subunit A) and 627 (subunit B) of PSI are especially important for maintaining this interaction [10, 25]. Furthermore, it has been shown that a small change in Pc's hydrophobic patch, such as switching Leu12 to Glu, results in a 20-fold decrease in the binding and a 8 times slower electron transfer to PSI [26]. These studies emphasize the importance of conserved regions, both in PSI and Pc, in the design of complementary and correctly shaped binding sites.

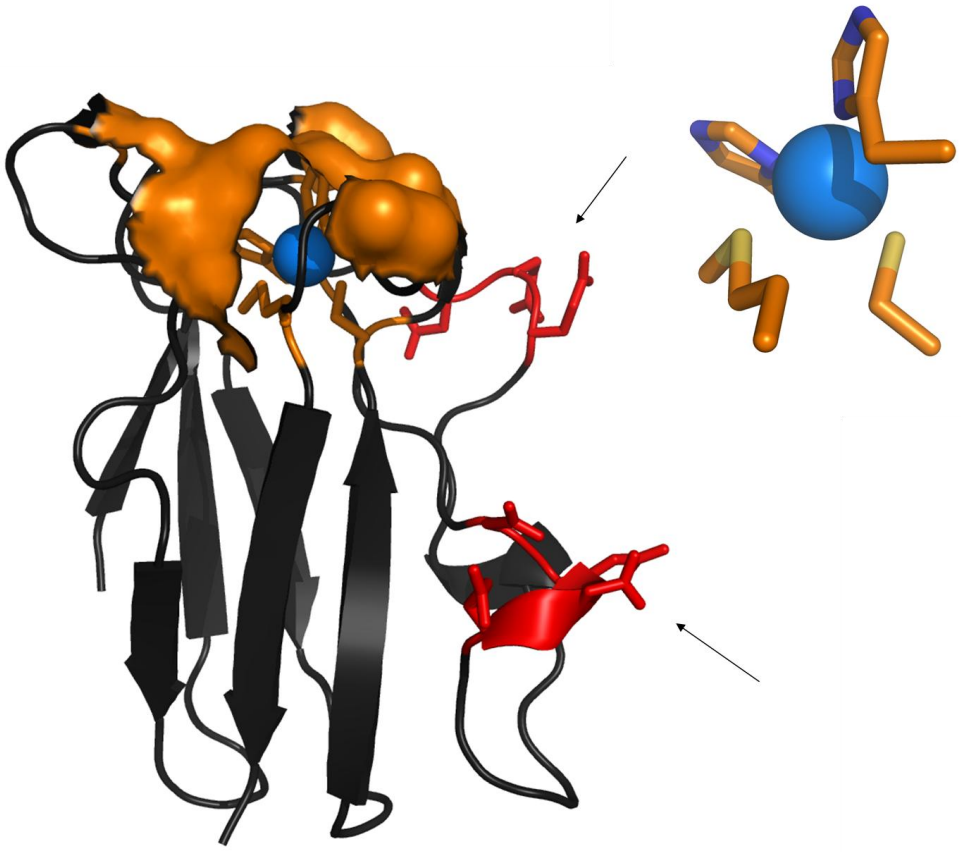

Figure 6: Cartoon representation of Pc. The surface is shown to emphasize the conserved hydrophobic patch (site 1). Amino acids 42-45 (lower patch) and 59-61 (upper patch), conserved in plants and green algae (site 2) are indicated with arrows. The bound copper and ligands (His37, Cys84, His87 and Met92) are shown in the upper right.

Site 2 has been shown to be important in stabilizing the complex formed between Pc and PSI, facilitating an efficient electron transfer to P700 [27]. Using mass spectrometry and chemical cross-linking, Hippler et al. showed that both the upper and lower acidic patches are involved

in the binding to the PSI subunit PsaF [28]. Furthermore, the report revealed that the lower acidic patch is involved in stabilizing the Pc-PSI complex through precise interactions with PsaF residues 10-24 but the exact residues could not be determined. Residues 10-24 includes some of the positively charged lysine residues found in the prolonged region of plant PsaF. The upper acidic patch, on the other hand, cross-links to PsaF residues in the region 24-51, which are also in the prolonged region of PsaF.

Transient binding of Pc to PSI

Protein interactions involving redox proteins are in general not very strong, but characterized by a rather low specificity and hence high dissociation constants (K_d-values) of the protein complex. There are several reasons for why evolution has designed this category of proteins in this fashion. Multiple interaction partners in an electron-transfer chain (such as Pc binding to both cytochrome b_6f and PSI) restrict a protein to be too selective for a certain partner since otherwise it would lead to a low turnover rate and to the accumulation of harmful radicals.

Hence, the physical properties of this group of proteins have evolved towards what is usually called transient binding. To describe the transient interactions often found between electron-transfer proteins, a so-called Velcro model has been introduced (Fig. 7, where $K_d = k_{off}/k_{on}$, $k_{on} = k_1k_2/(k_{-1}+k_{-2})$, $k_{off} = k_{-1}k_{-2}/(k_1+k_2)$) [29] in which special attention is paid to the initial assembly of binding modes. Many orientations of so-called encounter complexes are initially formed, all of which have somewhat overlapping binding sites. The formations of encounter complexes are strongly driven by long-range electrostatic interactions followed by a dipolar-driven pre-orientation before the contact. Once inside the same hydration shell, a high sampling rate between orientations is attained due to high rotation rates and lateral diffusion. Hence, this Velcro-like formation of encounter complexes results in a high k_{on}. However, once in the active complex, short-range interactions such as H-bonds, van der Waal and hydrophobic contacts, are more important to govern specificity. Yet, these later types of interactions should not to be too strong in order to attain a high k_{off}. In reality, the hydrophobic regions are often quite small, for example, Pc's hydrophobic patch is ~500 $Å^2$ compared with ~1500 $Å^2$ for typical antibodies [30]. Furthermore, the hydrophobic region is often surrounded by charged residues which in turn leads to the protein not being too tightly bound. In fact, it has been shown that the instant change in redox state following the electron

transfer can alter the affinity for some protein-complexes [31]. Combining these effects, a large k_{on} and a relatively large k_{off} can be maintained, resulting in a high turnover. This model differs significantly from the traditional lock-key model where interaction partners generally form stable complexes with drastically reduced turn-over [29, 32-36].

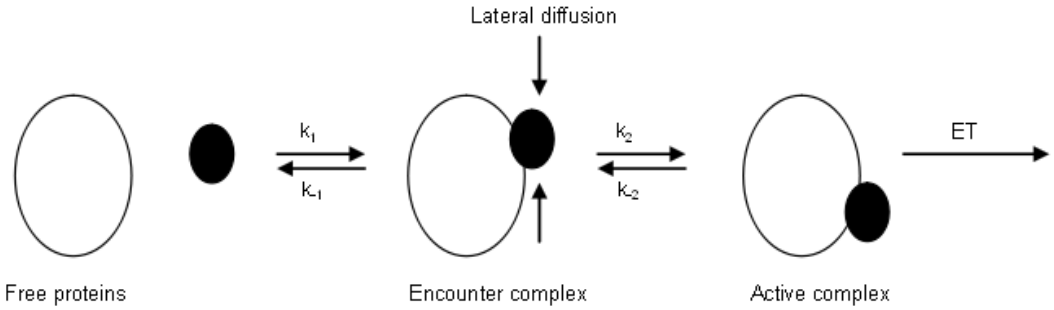

Figure 7: Reaction scheme of the Velcro model showing a two-step reaction involving an encounter complex followed by conformational rearrangement via lateral diffusion to achieve the active complex.

In plants, and in the case of electron donation from Pc to PSI, flash-induced transient absorption experiments reveal a biphasic reduction of the special pair $P700^+$ chlorophyll in the presence of reduced Pc. The two components represent two different events. The fast component with half-life of approximately 13 µs corresponds to Pc bound to PSI in an active conformation. Thus, upon illumination, the rate of electron transfer to $P700^+$ is monitored. The second component, with half-life of the order of several hundred microseconds, corresponds to the fraction of Pc molecules which experience the entire process of first binding to PSI, possibly undergoing conformational rearrangement, followed by electron transfer to $P700^+$ [37].

The electrostatic interactions involved in the formation of encounter complexes are strongly dependent on pH and ionic strength. This is interesting from a regulatory point of view since both factors are modulated during the dark-light transitions in oxygenic photosynthesis.

The role of magnesium ions in oxygenic photosynthesis

Illumination of chloroplasts leads to a transport of Mg(II) ions out of the lumen through a voltage-dependent cation-selective channel [38]. Since the chloroplast envelope is essentially

impermeable to Mg(II), the concentration of free Mg(II) increases with 1-3 mM in the stroma [39]. Together with a pH increase in the stroma and Trx-mediated cleavage of disulphide bonds in certain Calvin-cycle enzymes, this leads to a stimulation of CO_2 fixation. The estimated drop in free Mg(II) within the lumen is from ~10 mM to a few mM upon illumination [Paper II]. Hence, if proteins within the thylakoid lumen bind Mg(II) with K_d of the order of a few mM, this could act as a means of regulation [40].

A Mg(II) dependency has been documented for the electron donation to PSI which cannot be ascribed to a simple ionic strength effect [41-44]. In fact, the electron transfer from Pc to PSI depends strongly on the divalent cation, suggesting a specific binding to Pc. A skewed bell-like dependence has been noted with an optimum around 5 mM and half-maximal rates at 1 mM and 30 mM. Hence, the estimated changes in free Mg(II) content described above suggest that the Pc-PSI interaction is regulated *in-vivo* by Mg(II). This is the topic of Paper II in this thesis.

The role of thioredoxin in oxygenic photosynthesis

Thioredoxins (Trx) are 12 kDa proteins, found in all cells from bacteria, yeasts, plants to mammals, that are involved in disulphide-exchange reactions. They have a major role in redox regulations of proteins. Examples are many, such as enzymes of the Calvin-cycle (in photosynthesis), in the respiratory chain (in mitochondria) and in transcriptional regulation. Reduction of disulphide bonds may have structural implications on Trx target proteins. For example, this could deactivate an enzyme by affecting its stability and protein fold. It could also be the other way around, a target enzyme covalently locked in a non-productive conformation stabilized by disulphide bonds, could be activated upon reduction by Trx. In the Calvin-cycle, enzymes involved in CO_2 fixation are activated by the reduction of disulphide bonds, during the so-called dark-light transition. There are many different homologues of Trx, however all have the same conserved active site (WC[G/P]PC) containing two cysteine residues which are involved in exchange reactions with target disulphides. Crystal structures of Trx from different organisms show strong structural resemblance [45-49].

Although Trx is found in almost all organelles and their compartments, few studies to date have addressed its presence in the thylokoid lumen [50, 51]. FKBP13, a disulphide-bond-

containing immunophilin found in the thylokoid lumen, is known to be deactivated upon reduction by Trx [50]. Recently, a membrane-anchored Trx-like protein called HCF164 was discovered. HCF164 contains the Trx-conserved CXXC domain exposed to the thylakoid lumen. In the mentioned study, Trx-m *in-vivo* located in the stroma, was shown to transfer reducing equivalents to HCF164 on the luminal side. How this is made possible is not exactly known. The transfer is speculated to occur through a plant homolog to prokaryotic DsbD, in analogy with bacterial redox signaling between cytoplasm and periplasm [52].

Interestingly, HCF164 has also been shown to target the PSI subunit PsaN [52]. PsaN, which is only loosely bound to the luminal side of PSI, is known to modulate the interaction between Pc and PSI. When the gene is knocked out in *Arabidopsis*, the rate of electron donation to PSI is reduced by a factor two [53]. It has been suggested that PsaN stabilizes PsaF and indirectly facilitates a more efficient binding of Pc. In the crystal structure of PSI from pea, PsaN and likewise PsaF are in their reduced, thiolated, form. PsaN is located quite far from PsaF and the binding site of Pc [3].

Large-scale proteomics studies by [54] have revealed several new Trx-target proteins located within the lumen, many of which belong to PS II, but PsaN was also identified. However, since those studies were made on soluble proteins, little is known of membrane-bound proteins exposed to the thylakoid lumen such as PsaF. Hence, in large contrast to the thylakoid stroma, where enzymes are activated by Trx-mediated reduction upon illumination, recent reports suggest a Trx-mediated reduction and subsequent **inactivation** of lumen enzymes [51]. A likely explanation is that this occurs when chloroplasts return to a resting state in the dark. Then, when reducing equivalents are not longer needed in the stroma, they are transferred to the lumen, shutting off the system. When light is turned on again, molecular oxygen will be formed as a product of the water-splitting reaction at PSII. The resulting oxidizing environment in the lumen may then lead to reformation of disulphide bonds in certain proteins, reactivating the system. Indeed, it has recently been suggested that Cyt c_{6A}, and maybe also Pc, are involved in such oxidative processes [13]. In Paper III in this thesis it is shown that Trx can reduce the disulphide bond in PsaF, resulting in a protein with less ability to bind reduced Pc. However, oxidized Pc can restore the disulphide bond in PsaF, reactivating the protein. In the course of this thesis work it was planned to investigate the

possible role of the cysteines in PsaN. However, as described in Paper IV, it has so far not been possible to produce sufficient amounts of recombinant PsaN.

Angiogenin, another copper protein?

Angiogenin is a small (14 kDa) soluble protein belonging to the pancreatic ribonuclease (RNase) family and is a strong agent of blood-vessel formation. Originally found in carcinoma cell culture media, angiogenin has been shown to be important for neovascularisation in tumors as well as in non-malignant tissue [55].

Human angiogenin (hAng) has two identified modes of actions, both which are distinctively different from one another but necessary to attain angiogenic activity. First, hAng has a very weak ribonucleolytic activity, 10^5 times less efficient than ordinary RNase. Secondly, hAng has two transport sequences, the first one binds to endothelial cell-surface receptors which directs angiogenin to the cytoplasm and the second one is a nuclear localization sequence (NLS) which directs hAng to the cell nucleus.

X-ray and NMR structures reveal a protein composed of three alpha helices and three disulphide bonds and a catalytic site consisting of His13, Lys40 and His114 as can be found for other RNases. However, in hAng, the pyrimidine-binding pocket appears to be obstructed by Gln117 which may explain the low activity [55-60].

Soncin et al. [61] reported on an increased binding of hAng to pulmonary artery endothelial cells in the presence of Cu(II) and Zn(II). Other mono- and divalent ions showed no effect. Preliminary characterization of the Cu(II)-binding, using affinity chromatography and radioligand binding assays, showed on a 2.4 binding stoichiometry with one strong binding site (K_d~1 nM) and one weaker binding site (K_d~0.14 µM). A hAng–Cu(II) complex was characterized with UV-vis spectroscopy showing a weak absorption band at 725 nm [61]. Interestingly, Lee et. al reported on a Cu(II)-dependent inhibition of hAng ribonucleolytic activity. The results imply that Cu(II) is bound close to the catalytic site [62]. Hence, two different counter-acting effects have been documented: On the one hand, copper stimulates the transportation process, while, on the other hand, it decreases the enzymatic activity. This is strange since both processes are essential for hAng to attain its angiogenic activity.

In this thesis work, as a part of an international collaboration with the group of Diego La Mendola (University of Catania, Italy), we have characterized the copper binding to hAng. This is the subject of Paper V. Furthermore, some functional aspects of this interaction have been considered and are under current investigations.

Methodology

Strategies for protein expression

In this work, *E. coli* has been used as expression host for producing Pc and the PSI luminal domain of PsaF, PsaN and hAng, due to its flexibility, robustness and the possibility to isotopically enrich the proteins. The flexibility arises from the large variety of tools made available through the development of modern molecular biology which facilitates the construction of recombinant DNA. Techniques have also been developed at different stages to enhance the expression of functional proteins, all which in the end affect the yield and state of the final product.

In *E. coli* strong correlation between mRNA levels and protein expression is well established. Hence, different ways of increasing the number and life time of mRNA have been developed. However, the most reliable and effective way to alter the transcription and the mRNA levels is by means of a strong inducible promotor. The T7 promotor, originating from bacteriofag T7, offers the high levels of transcription and stringent control that is not found for *E. coli*-based promoters such as *lac*UV5, which are under the control of the lac operon. This efficient transcription is attained through the T7 RNA polymerase. A tight regulation of transcription is often preferred since even a small basal level (or 'leaky') of expression may be toxic for the cells. To utilize the T7 promoter in vectors such as in the pET vector series, the plasmid needs to be transformed into a host that has a chromosomal gene encoding for T7 RNA polymerase, such as a BL21 (DE3)-derived strain [63]. The gene for T7 RNA polymerase is often under *lac*-control and hence the expression of T7 RNA polymerase is induced by the addition of IPTG (isopropyl-beta-thiogalactoside) and subsequently the recombinant protein is expressed.

To alter the level of translation is a more challenging task since more factors influencing post-transcriptional expression levels are present in comparison to the transcriptional process. The usage of *E. coli*-preferred codons, or so-called codon optimization, can increase the translational rates of heterologous (non-*E. coli*) genes and decrease premature termination and truncation products due to translation-pauses that are inflicted by the presence of some rare codons [64, 65]. Alternatively, one can use the *E. coli* strain Rosetta, which contains an extra plasmid encoding for exotic tRNA's that are mostly found in eukaryota [66]. Strategies

involving gene fusion with a high-expressing nucleotide sequence attached through the flanking 5' end to the target gene, have also shown to be fruitful, most likely due to a more successful translation initiation.

A major obstacle following the translation is proteolysis, where heterologous proteins often fall victim for protein degradation. Proteases may target partly folded or dynamic proteins due to their higher degree of exposed regions which are susceptible to protease-mediated peptide hydrolysis. Some N-terminal residues are also more susceptible to degradation, such as Arg and Lys, due to posttranslational modification. To prevent this type of proteolysis, one may co-express the gene with a chaperone/foldase or an interaction partner, which may facilitate a faster folding and increase the stability of the gene product. Another approach is to "camouflage" the N-terminal end with a fusion protein originating from *E. coli* and with a well documented long half-life [67]. Expression at low temperature can also be an alternative, in order to lower the activity of proteases.

In many cysteine-rich proteins, disulfide bonds are essential to maintain a global fold and activity. To attain correct disulfide bonds and minimize degradation, one may direct the protein product to the periplasm via transporter peptides such as the OmpT and pelB leaders. In comparison to the *E. coli* cytoplasm, the periplasm is a more oxidative environment and may facilitate the oxidation of cysteine thiols to form disulfide bonds. One may also obtain similar results by fusing the target gene to thioredoxin (TrxA) and over-express in a *E. coli* TrxB/gor mutant strain (TrxB=thioredoxin reductase, gor=glutathione reductase). This mutation disrupts the cytoplasm disulphide metabolism by keeping TrxA oxidized and hence available for catalyzing the thiol-disulphide exchange reaction with the target protein [68]. However, precaution is recommended due to the drastically reduced growth rate of these strains. An exogenous source of reductant like DTT is often required to maintain growth.

When the efficient T7 promotor is used in *E. coli* it is common that insoluble protein-aggregates, so-called inclusion bodies are produced. The aggregated protein is in general described as being trapped in an intermediary fold, and is not functional for most proteins. To circumvent this problem one may alter factors that lower the expression rates or facilitate the folding [69]. Sometimes the expression is deliberately aimed towards producing inclusion

bodies. Strategies of this sort try to benefit from the very high yields and little degradation usually obtained with protein produced in inclusion bodies. However, then one needs to develop and optimize refolding procedures in order to obtain a functional protein.

To simplify purification, one may insert a nucleotide sequence, 6xCAT flanking the gene to be expressed. This sequence codes for an N- or C -terminal His_6-tag which binds divalent transition metals such as Ni^{2+} with high affinity. This property is further exploited in affinity chromatography (see section below).

The Polymerase Chain Reaction and techniques for molecular cloning

The Polymerase Chain Reaction (PCR) revolutionized the field of molecular biology by making it possible to isolate and amplify a fragment of DNA from a complex mixture with a very high accuracy but only using very small amounts of starting material [70]. The procedure enables the possibility to isolate a certain gene at a quantity sufficient to be cloned into a host organism. Combined with a creative usage of restriction enzymes one can tailor expression vectors to include certain functional elements (promotors, protease sites etc) together with the gene to be expressed. PCR is an *in vitro*-based technique which has a strong analogy with DNA replication *in vivo*. Similar ingredients are included such as DNA primers, which are small complementary synthetic oligonucleotides flanking the gene of interest, template DNA, dNTP, thermostable DNA polymerase, and buffer conditions that serve to stabilize the DNA (with co-factors and DNA polymerase). The method is based on thermal cycling, and the procedure includes the following steps: 1) Thermal denaturation of template DNA (T~95ºC). 2) Annealing of primers to single-stranded template DNA (T~Tm~55ºC). 3) Extension with help of DNA polymerase (T~72ºC). Steps 1-3 are cycled to yield sufficient amounts of amplified material. Each new cycle generates a new set of templates, hence the amount of product will increase exponentially (2^{n-1}, n = number of cycles). Due to the restraints set on the reaction conditions by the thermal denaturation (step 1), only thermally stable DNA polymerase can be used such as Taq polymerase or any of it derivatives. Taq polymerase was originally discovered from *Thermus aquaticus*, a bacterium found living in hot springs [71, 72]. Pfx and Pfu DNA polymerase can also be used to give an even higher accuracy, due to

their proofreading 3'-5' exonuclease activity (see Site-directed mutagenesis), giving an even lower frequency of base-pair mismatching.

Ligation-independent cloning (LIC) is a directional cloning strategy. By utilizing the T4 DNA polymerase 3'->5' exonuclease activity, in the presence of a single nucleotide specie (dGTP), complementary overhangs on both the PCR product and the linearized expression vector can be obtained. The procedure is very specific and yields few false positives since only the annealed product (which generate nicked circular DNA) will be susceptible for transformation and subsequent ligation within the cell. This procedure does not require ligation reactions or digestion by the use of additional restriction enzymes to attain the final product [73].

Sticky-end cloning is accomplished by treating the amplified DNA and the plasmid with restriction enzymes, generating complementary overhangs of ~4-6 bases in length. The technique is directional since the complementary overhangs of PCR product and plasmid vector have only one possible orientation. Hence the method is superior to blunt-end cloning, where the PCR fragment can anneal in two different orientations with respect to the plasmid. Furthermore, self-ligation is avoided.

Site-directed mutagenesis

Site-directed mutagenesis can be used to investigate what influence a single (or several) amino-acid residue may have on the functional activity or folding of the protein at hand. By changing to Trp or Cys residues one can introduce markers, fluorescent or paramagnetic. Sometimes the goal is to explore the binding interface of two proteins. In these cases, residues thought to be important for electrostatic interactions are neutralized or modified in a way that fits the scope of the study.

QuickChange^{TM} Site-Directed Mutagenesis is a technique that has been developed to introduce mutations/deletions with very high accuracy. The general procedure consists of: A) Thermal cycling B) Selection C) Transformation and ligation. The thermal cycling includes three steps: 1) Thermal denaturation, exposing regions of potential annealing to the primers. 2) The two complementary primers including the desired mutation are annealed to the parental template DNA. 3) Extension with high fidelity Pfu DNA polymerase. The steps 1-3

are repeated as for an ordinary PCR. However in this case only the parental DNA is used as template in each new cycle. Hence, only a linear increase of product with the number of cycles will be obtained. This procedure minimizes the risk of amplifying mismatches and generating false positives. Following temperature cycling, the mutated plasmid is selected by treating the product with DpnI. The DpnI endonuclease is active towards methylated DNA and hence will digest the parental template DNA [74]. The nicked plasmid is transformed into competent *Epicurian coli* XL1-Blue cells where the plasmid is ligated. The mutations are commonly verified by DNA sequencing.

Purification and general chromatography

Lysis of bacterial cells is often accomplished by standard means. With a French press one can disrupt cell walls mechanically by passing the cells through a narrow passage under the influence of a high static pressure. The cell walls are gritted apart by shear forces as the cells expand when exposed to atmospheric pressure. The same result can be accomplished biochemically by treating the cells with lysozyme. This enzyme catalyzes the hydrolysis of the peptidoglycan mesh-like network of the cell wall, hence solubilizing it and exposing the interior of the cell [75]. Centrifugation is often used to separate soluble fractions from insoluble, such as leftover debris of membranes and inclusion bodies that are obtained after cell lysis.

Once a clear lysate has been obtained, purification is accomplished by chromatography. A brief description of the three most common techniques is given here. Affinity chromatography utilizes a specific property of the protein at hand, such as ligand binding or binding to a protein interaction partner. In the present work, Immobilized Metal Affinity Chromatography (IMAC) has been utilized to selectively purify His_6–tagged proteins. The metal-chelating matrix of the IMAC can be loaded with different divalent transition metals such as Ni^{2+}, Cu^{2+}, Zn^{2+} or Cd^{2+}. In principle, the technique exploits the high affinity of the metal-coordinating complex formed between the metal ion and the imidazole rings of the His_6-tagged protein [76]. Once the protein has been eluted from the column via substrate competion (by adding large quantities of imidazole) the His_6-tag can easily be removed through specific proteolysis with a suitable protease (such as factor Xa or TEV) to retrieve the correct N-terminal end of the protein.

Ion-exchange chromatography and size-exclusion chromatography (SEC) are more traditional tools of protein chromatography. Ion-exchange resins can be positively or negatively charged and the separation is based on the isoelectric point (pI) of the protein at hand. The net charge of the stationary phase is set by equilibration with buffers of suitable pH which will lead to a binding of the target protein. In analogy with affinity chromatography, the protein is released from the matrix by increasing the ionic strength in an appropriate manner. In SEC, separation is accomplished by restricting the migration path of the differently sized proteins by passing the mixture through a stationary phase with variable pore size. Small proteins will have the option to diffuse through a larger number of pores and hence will have a longer migration path in comparison to larger molecules, leading to a separation.

Characterization of isolated proteins

Chemical cross-linking

N-ethyl-3-[3-(dimethylamino)propyl]carboiimide (EDAC) is a zero-length cross-linking agent. The cross-linking between biomolecules with EDAC is a two-step process: First EDAC reacts with surface-exposed carboxyl groups forming an unstable amine-reactive intermediate (O-acylisourea). This will quickly react with any nearby amino groups to form an amide bond between the two and the release of isourea.

In order to be sure that no unspecific cross-linking will occur except between carboxyl groups on one protein and amine groups on another, one need to have a control. The idea behind the control cross-linking reaction is to block the reactive carboxyl groups on the first protein through chemical modification. This chemical modification is done by cross-linking the carboxyl groups with the amine group of glycine ethyl ester (GEE) in the presence of EDAC.

The above procedure has shown to be very successful in trapping initial encounter complexes that are strongly driven by electrostatic interactions. Crnogorac et al. used EDAC to trap encounter complexes of Pc and Cyt c [77]. Furthermore, in the study of Pc-PSI binding, Hippler et al. and Malkin et al. used EDAC to covalently attach Pc to PSI via the PSI subunit PsaF in a specific manner [7, 9].

Detection of free SH-groups using MIANS

Reduced cysteine residues can be detected via fluorescence labels. MIANS is a thiol-reactive fluorophore which shows a dramatic increase in fluorescence quantum yield upon conjugation in a nonpolar environment of a biomolecule [78]. The conjugation consists of a thioether link between the protein and MIANS. In a mixture consisting of two or more cysteine-containing proteins, one may isolate individual species by means of gel electrophoresis (SDS-PAGE). Monitoring the MIANS fluorescence will then make it possible to distinguish the specie(s) with free thiol groups.

Absorption and Fluorescence

Some molecules can absorb light in the UV-vis spectral range. At a certain wavelength, the electric-field component of the electromagnetic radiation will interact with the electronic structure of the molecule inducing an electric dipole and the transition to an excited state, a photon is absorbed. When in the excited state, energy may dissipate to the surrounding environment through different routes upon returning to the ground state. The molecule may reemit a photon via fluorescence or simply just transfer the energy to surrounding molecules by decaying through vibrational states (internal conversion) or by collision-induced quenching. Fluorescence emission occurs at a longer wavelength in comparison to light absorption. This is due to: 1) Following electronic excitation, rapid vibrational deexcitation occurs to the lowest vibrational state in S_1 (the first electronic excited state). 2) The contribution from the difference in reorganization energy, the so-called Stokes shift, appears due to the rearrangement of solvent molecules to "fit" the excited-state electronic structure. At the moment of excitation all nuclear coordinates are essentially stationary with respect to the redistribution of electrons (Born-Oppenheimer approximation). Hence, the energy level of the equilibrated excited state will be slightly lower than the initial excited state, since the surrounding adapts to the new excited state. The two contributions (internal conversion and Stokes shift) will add up and result in a smaller energy gap in comparison to the absorption process and hence a longer wavelength of the emitting photon. This is why one can excite a chromophore at one wavelength and detect at another [79, 80].

Both absorption and fluorescence of certain aromatic molecules such as Trp, Phe and other synthetic probes (MIANS, SYPRO Orange) can be used in different applications to study the polarity of the environment of the biomolecule. Under favorable conditions one may also

study enzymatic reactions or protein-protein interactions by probing the rate of accumulation of an absorbing or fluorescing product (or species).

Secondary structure composition investigated by CD

When illuminating a chiral molecule with circularly polarized light, the electrons of the molecule may interact differently with the electric-field component depending on if the light is left- or right-circularly polarized. A CD spectrum shows the difference in absorption between the polarizations, $A_{left} - A_{right}$.

In proteins, the peptide-bond amide transitions can be monitored by far-UV CD (190-240 nm), giving structural insight about the secondary-structure composition. Pure α-helical, β-sheets and random-coil structures have distinct spectral features within this region and an experimental CD spectrum of a general protein can be considered to be a linear combination of the three pure spectra. The relative portion of each structural element can be calculated from a minimum of three wavelengths, but an over-determined equation system becomes more accurate. One may also use a basis set that has been constructed from known protein structures and their secondary-structure composition to reconstruct experimental data. A benefit of the latter approach is that tertiary structural effects (packing of helices etc) are indirectly included since real proteins are used in the basis [80].

Changes in the secondary structure upon changing buffer conditions, mutations or addition of ligands can give valuable insight into the stability and function of the protein at hand.

EPR spectroscopy

An unpaired electron has a magnetic angular momentum due to the electron having an intrinsic spin S=1/2. Due to quantization, the magnetic angular momentum can adopt 2S+1 orientations in a magnetic field. Upon absorbing a microwave quantum, the resonance condition is: $h\nu=g\beta B_0$ for the transition S=-1/2 -> 1/2 (where the magnetic-field component of the EM-radiation induces the transition). Transition-metal ions such as Cu^{2+} and Mn^{2+}, and organic radicals containing unpaired electrons can be studied with EPR. The g-value obtained from an EPR spectrum reveals features about the environment of the unpaired electron. If a nuclear spin is within close proximity to the electron, the EPR spectrum may give information

about this. Energy splitting, so-called hyperfine splitting, occurs due to the change in the local magnetic field that is felt by the electron from the different orientations of the close-by nuclear spin. The hyperfine-coupling constant A, is a useful quantity that can help identifying an EPR-active molecule.

NMR spectroscopy

In analogy with EPR, NMR is the study of nuclear spins in an applied magnetic field. In biomolecular NMR, spins of I=1/2 such as ^{1}H, ^{13}C and ^{15}N are of particular interest, since recombinant protein expression in *E. coli* facilitates a relatively inexpensive production of isotopically enriched samples. In NMR the resonance condition is given by $\omega=-\gamma B_0$ (in $rads^{-1}$), where ω is the Larmor frequency and γ is the magnetogyric ratio. For a particular nucleus in a protein, the local chemical environment will influence the effective magnetic field experienced by that nuclei, resulting in a slight change of the Larmor frequency. This so-called chemical shift will be an ID-tag for that particular nucleus. In this work the main concern has been to study protein-protein (or protein-ligand) interactions. Hence the concept of chemical exchange will be described below. Paramagnetic NMR has been used to investigate the transient protein-ligand complex Pc-Mn(II), and some of the major concepts will also be mentioned below.

Chemical exchange

The following reaction represent a symmetric two-state chemical exchange, for example a conformational change of a molecule:

$$A \underset{k_B}{\overset{k_A}{<->}} B$$

$k_{ex}=k_A+k_B, \quad k_A=k_B$

Fast exchange ($k_{ex}>>(\omega_A-\omega_B)$)

This occurs when the rate of exchange (k_{ex}) between states A and B is so rapid that the time spent in one state is too short to be able to sample the precession of the spin being purely in that state. Instead, the rapid switching between A and B will give rise to a time averaged chemical shift. In a rotating frame precessing with the frequency ($w_B+dw/2$), one can imagine

that the transverse magnetization of the two states A and B will precess in different directions (clockwise and counter clockwise) about the rotating frame. If the exchange is symmetric ($k_A=k_B$) where 50% of the starting population is in A and B, the frequent switching between A and B will make the starting population A move towards B and the starting population B move towards A as time proceeds. Since it is symmetric exchange, they will meet half ways and the resulting signal will be centered between A and B.

Slow exchange ($k_{ex}<<(\omega_A-\omega_B)$)

A slow exchange between A and B will results in two peaks at ω_A and ω_B since each state will be populated long enough to be sampled. Hence, each integrated peak will be proportional to the corresponding concentration.

Ligand binding and chemical-shift perturbation

For a simple bimolecular binding of a ligand: A+L↔AL, chemical-shift changes are defined as being in the fast exchange regime on the Larmor frequency time scale if $k_{ex} = k_{off}+k_{on}[L] >> \omega_A-\omega_B$ (A = free protein, B = ligand-bound protein) and the observed peak will be the population-weighted peak of both A and B. The relative change in the chemical shift can be used to extract the dissociation constant ($K_d=k_{off}/k_{on}$) for the binding of the ligand [81].

Paramagnetic relaxation enhancement (PRE)

The relaxation enhancement Γ_{2para} of a proton due to the strong magnetic dipole-dipole coupling introduced by a paramagnetic species like Mn(II) can be described by the Solomon-Bloembergen equation (eq. 1) for transverse relaxation.

$$\Gamma_{2\,para} = \frac{1}{15}\left(\frac{\mu_0}{4\pi}\right)^2 \gamma_I^2 g^2 \mu_B^2 S(S+1)\{4J_{SB}(0) + 3J_{SB}(\omega_I)\} \qquad (1)$$

Here, S is the electron spin quantum number, g is the g-factor of the electron spin, γ_I is the gyromagnetic ratio of the proton, μ_0 is the permeability of vacuum, μ_B is the electron Bohr magneton and r is the distance between the unpaired electron and the proton. The spectral density function (eq. 2) represents the actual spectral width of the different fluctuations and to what extent they are active in inducing the observed relaxation.

$$J_{SB}(\omega) = r^{-6}\frac{\tau_c}{1 + (\omega\tau_c)^2} \qquad (2)$$

The effective correlation time τ_c shown in (eq. 3), consists of three terms, τ_{rot}, τ_S and τ_{ex}. The modulation of the local magnetic field by molecular tumbling is characterized by τ_{rot}, the rotational correlation time of the protein-ligand complex. Relaxation induced via the dipolar coupling to an unpaired electron spin is represented by τ_S, the electron spin relaxation time. The contribution of chemical exchange is usually negligible and hence can be omitted from (eq. 3).

$$\frac{1}{\tau_c} = \frac{1}{\tau_{rot}} + \frac{1}{\tau_S} + \frac{1}{\tau_{ex}} \qquad (3)$$

From a practical point of view, Mn(II) derived paramagnetic probes have one major advantage compared to other paramagnetic probes in interaction studies. The isotropic g-tensor of the Mn(II) electron system greatly simplifies the analysis since only PRE's and no pseudocontact shifts have to be considered (ω_A-$\omega_B \approx 0$). Therefore, time consuming reassignments are not required.

The observed line width will be given by:

$$\Gamma_{2\,obs} = \Gamma_{dia} + p_B\Gamma_{2\,para} \qquad (4)$$

Here p_B is the fraction of proteins with a bound ligand. To calculate the observed line width, p_B needs to be calculated as well as Γ_{2para}. By using complementary experiments (EPR or NMR), K_d-values can be obtained which in turn can be used for calculating p_B.

Results and Discussion

Cloning, expression and purification of the luminal domain of spinach photosystem 1 subunit PsaF functional in binding to plastocyanin and with a disulphide bridge required for folding (Paper I)

A major objective with my project as a whole has been to investigate the protein complex formed between Pc and the lumen-exposed domain of the PSI subunit PsaF. The early cross-linking and mutagenesis studies by Hippler et al. [11] and Young et al. [27] had shown that this domain is the site for precise recognition by Pc. Therefore, this was thought to be a good starting point for structurally characterizing the initial Pc-PSI protein complex. In order to do so, a procedure to purify the lumen-exposed domain of PsaF was needed. In this first paper, we report on the expression and characterization of this domain, in the following text referred to as PsaF´.

Initial trials to express PsaF´ showed to be unfruitful. The domain had a strong tendency to be proteolytically degraded within the *E. coli* cytoplasm, or expressed as inclusion bodies when fused to transporter peptides. By pure luck, we encountered Tom Wydrzynski who tipped us about the Trx-fusion system.

As described in detail in Paper I, expressing PsaF´ in fusion with Trx and subsequent purification results in approximately 6 mg of purified protein sample per liter of culture media. The progress of the preparation is conveniently shown with a Coomassie-stained gel (Fig. 8).

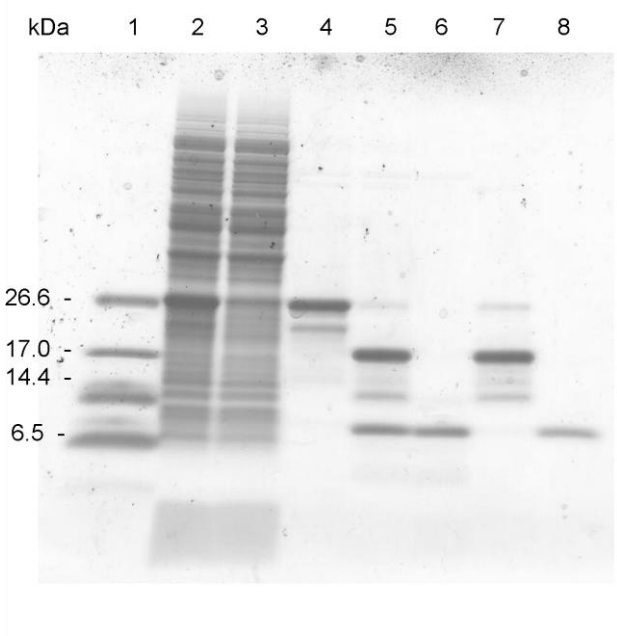

Figure 8: SDS-PAGE following the progress of a typical purification of PsaF´. Lane 1: Mw standard, lane 2: soluble cell lysate, lane 3: non-bound protein after IMAC no. 1, lane 4: purified fusion protein after IMAC no. 1, lane 5: purified fusion protein treated with factor Xa, lane 6: non-bound protein from the flow-through of IMAC no. 2, lane 7: elutant from IMAC no. 2, lane 8: final purified PsaF after SEC [see Paper I].

The PsaF´ secondary structure was early characterized by CD, revealing spectral features consistent with typical alpha-helix-containing proteins, with two negative peaks at 222 nm and 207 nm followed by a large positive peak at 191 nm (Fig. 9 right). Thermal-denaturation studies with CD revealed a fully reversible and rather low helix-coil transition temperature at 29 ºC, with only a small degree of cooperativity (Fig. 9 left). When investigating the effect of the alcohol-based cosolvent trifluoroethanol (TFE), a strong propensity to form helix structure could be noted already at low amounts of TFE (Fig. 9 right).

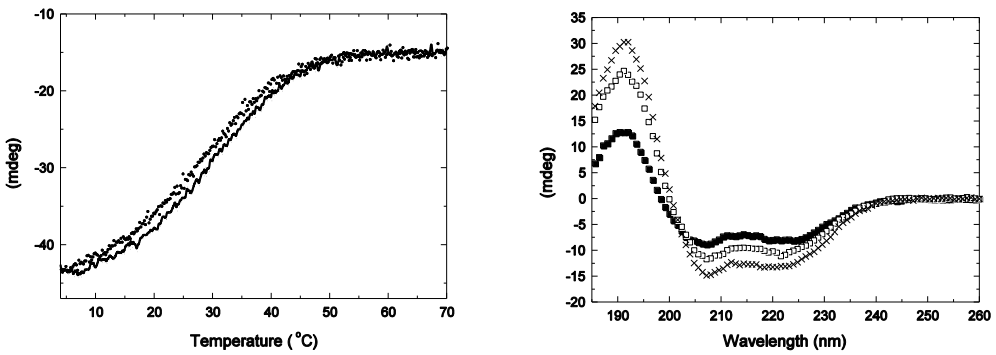

Figure 9: Left) Thermal denaturation of PsaF´ monitored by CD at a fixed wavelength of 220 nm [see Paper I]. Right) Far-UV CD spectrum of PsaF´ at 4 ºC with gradually increasing amounts of TFE, going from 0% (filled squares), 25% (open squares) and 50% (crosses).

Further characterization using a fluorescence-based thermal-shift assay, thermofluorescence (TF), gave different results (Fig. 10). The data are consistent with a protein domain with a stable hydrophobic core, which only becomes exposed to surrounding solvent above 50 ºC.

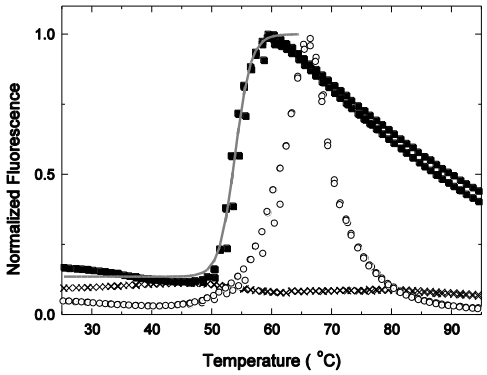

Figure 10: Thermofluorescence measurements of PsaF´ (filled squares), PsaF´ in presence of DTT (crosses) and oxidized Pc (open circles). The excitation and emission wavelength were 470 nm and 530 nm, respectively [see Paper I].

At first, the CD and fluorescence measurements appeared contradictory. However, much became clear when it was realized that the two helices are inter-connected by a disulphide bridge (Cys8-Cys63), as confirmed first by TF and later by MS. The disulphide bridge is a requirement for the domain to maintain its hydrophobic core and tertiary fold (Fig. 10).

The redox state of Cys8 and Cys63 was an open question from the start. The reason for this was that the first high-resolution PSI structure from a plant source (pdb 2o01) [4], as well as the very recent structure from the same group (pdb 3lw5), reveal that the two cysteine residues are in their reduced state. However, in the cyanobacterial counterpart, the cysteine residues form a disulphide bridge [10]. Our results in Paper I show clearly that the disulphide bridge is intact under natural (oxidizing) conditions.

In conclusion, the different results from CD and TF reflect the inhomogeneity of structural features within this domain. One way to describe this is by saying that there is one region (in which Cys8 and Cys63 are found) which is more hydrophobic in its character and which is monitored in the TF experiment. Then there is the second region, consisting of the helix-turn-helix motif with a more sparse distribution of hydrophobic residues, which is not detectable

with TF, plausibly due to a low degree of incorporation or a high degree of solvent exposure of the fluorophore. The later region, detectable by CD, displays regular yet dynamic secondary-structure features. Overall, the domain seems to belong to the molten-globular structural family. This interpretation is further supported by the small chemical-shift dispersion noted for the NMR ^{15}N-HSQC spectra of ^{15}N-PsaF´ and the slow/intermediate chemical exchange giving rise to extra peaks and severe line-broadening effects [see paper I].

Site-directed mutagenesis combined with cross-linking studies of both PsaF´ and Pc results in similar interaction patterns as previously reported by Hippler et al. for the intact PSI protein complex [11]. The results highlight the importance of PsaF´ lysine residues K16 and K23 and lower acidic-patch residues (42-45) of Pc for an efficient binding (Fig. 11) [see Paper I and Paper III]. These results indicate that Pc binds to PsaF´ in a manner which has much resemblance to the initial binding of Pc to PSI.

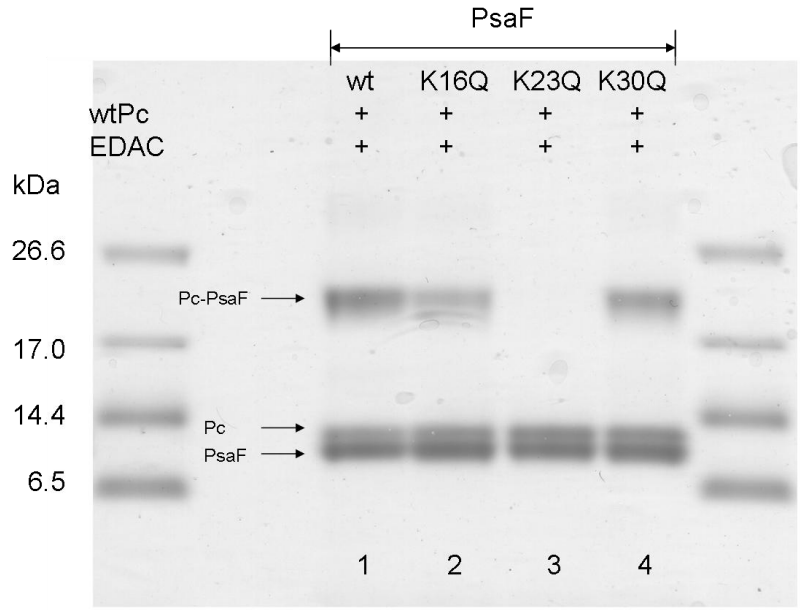

Figure 11: SDS-PAGE with cross-linking setup as indicated in the upper part of the figure. Reduced Pc and PsaF´ mutants were present at equimolar amounts. PsaF´ mutants where expressed using a modified procedure where the original Xa-site had been substituted for a TEV-site (see Paper III).

A paramagnetic NMR study elucidating the binding of Mg(II) and Mn(II) to spinach plastocyanin. Regulation of the binding of plastocyanin to subunit PsaF of photosystem I (Paper II)

In this paper, we investigate whether light-induced changes in the Mg(II) content in the chloroplast lumen can modulate the binding of Pc to PsaF. Initially, the idea of making this study came from screening buffer conditions for studying the binding of PsaF´ to Pc with 2D-NMR spectroscopy. Early buffer conditions were based on *in-vitro* flash-induced transient absorption measurements of the Pc-PSI electron-transfer reaction. In these experiments, a few millimolar of Mg(II) ions were always present. The addition of Mg(II) had an empirical origin, but the explanation for this additive was not entirely clear. However, it was not until Mg(II) was excluded from the buffers that a detectable binding of PsaF´ to Pc could be observed by NMR.

To study the inhibitory effect of Mg(II) on the Pc-PsaF´ binding, we first determined the individual binding constants for both Mg(II) and PsaF´ to reduced Pc (Pc^{red}), resulting in the dissociation constants 4.9 mM and 1.4 mM, respectively (Fig. 12). From the ^{15}N-HSQC of the Pc-PsaF´ complex, a competitive effect could be noted when gradually adding Mg(II). This addition resulted in a transition from the PsaF´-induced Pc spectrum to the Mg(II)-induced Pc spectrum. From these data we could extract an apparent dissociation constant for the Pc-Mg(II) complex, and from this we became certain that Mg(II) and PsaF´ bind to the same site on Pc, thus explaining the inhibition.

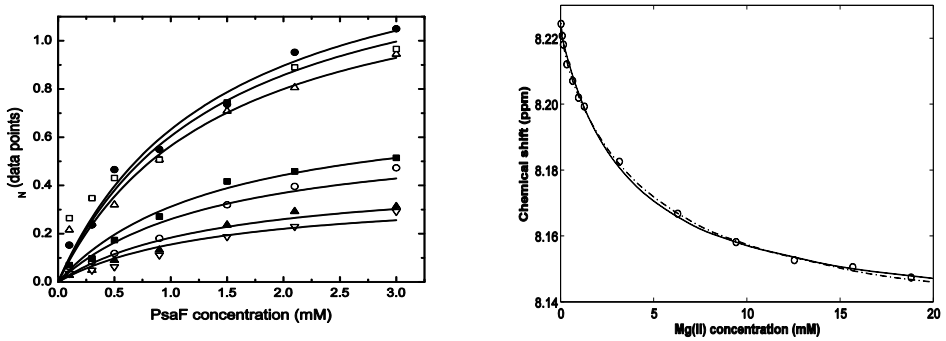

Figure 12: Chemical-shift perturbations measured from the Pc ^{15}N-HSQC spectra. Left) ^{15}N-shifts of the Pc back-bone amide groups: E45 (filled squares), I46 (filled circles), I55 (open circles), M57 (open inverted triangles), E60 (filled triangles), K81 (open circles) and G94 (open triangles) upon the addition of PsaF´. A single hyperbolic function was fitted to the data using a global fitting procedure resulting in a dissociation constant of 1.4 mM for the Pc/PsaF´ complex. Right) The binding of Mg(II) to Pc, monitored by the gradual

chemical-shift changes for back-bone amide proton K81 (open circles), upon the addition of Mg(II) to Pc. The chemical-shift perturbations were fitted with one and two hyperbolic functions, full line and dot-dashed line, respectively. For a one-site binding model, a dissociation constant of 4.9 mM for the Pc/Mg(II) complex was obtained [see Paper II].

We wanted to structurally elucidate the complex formed between Pc and Mg(II) and to do this we used the paramagnetic analogue Mn(II). By using the Solomon-Bloembergen equation to describe the line-width changes induced by the bound Mn(II), distances could be derived between the bound Mn(II) ion and the affected back-bone amide protons. Experimental line-width changes as a function of calculated distances are shown in Figure 13 for the best-fit location of the Mn(II) ion. To account for a small but notable line-broadening effect, so-called solvent PRE, a distance-independent contribution was included as an empirical constant (eq. 18 Paper II).

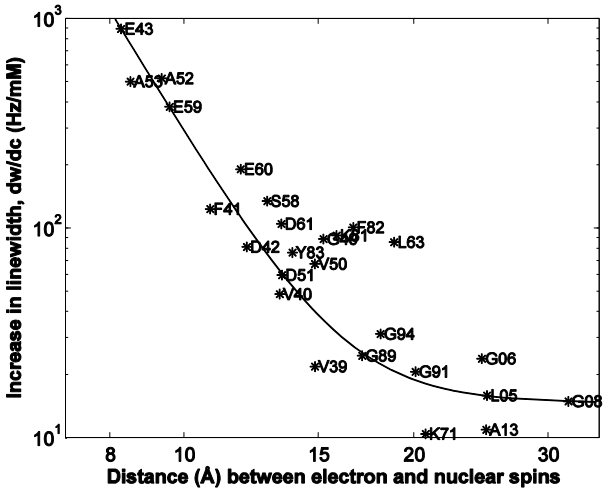

Figure 13: The concentration-dependent increase in ^{1}H line-width for the 25 indicated back-bone amide groups of Pc. The location of the bound Mn(II) ion was found from a grid search where the modified Solomon-Bloembergen equation (Paper II eq.18) was fitted to the experimental data. The coordinates for the bound Mn(II) were determined to (3.7, 57.4, 14.6)Å in pdb 1ag6.

The bound Mn(II) ion was found to be located close to the lower acidic-patch residue E43 (Fig. 14). The transient binding characteristics of Mn(II) suggest that the ion is bound as a hexaquo complex embedded within the hydration shell of Pc. The lower acidic patch is very important in the binding of PsaF as shown in this study, but also by site-directed mutagenesis [27]. Hence, binding of Mn(II) or Mg(II) to this region should result in an inhibition of the binding of Pc to PsaF.

It has been estimated that the change in free Mg(II) content within the thylakoid lumen drops from 10 mM to a few mM during the dark-light transition (see Paper II). This span in free Mg(II) content covers the K_d of the Pc-Mg(II) complex (K_d ~5 mM). Thus, a significant modulation of the electron donation from reduced Pc to PSI is plausible *in-vivo*.

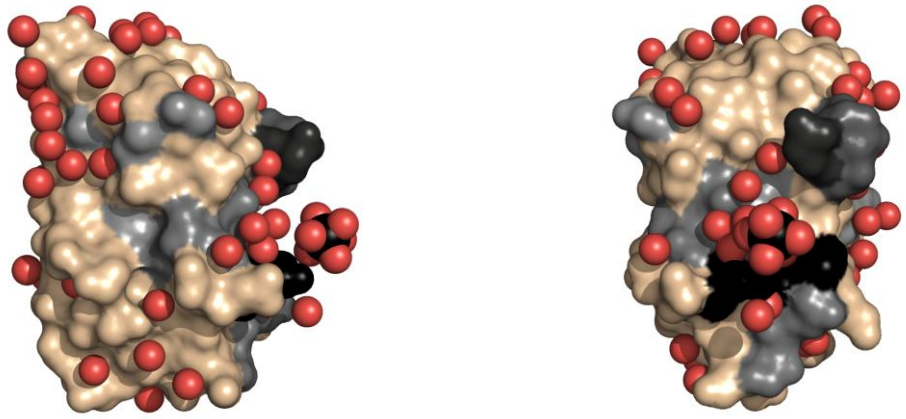

Figure 14: Left) The resulting PRE-based structure for the Pc-Mn(II) hexaquo complex. The surface representation of Pc including crystallographic bound water from pdb 1ag6 is shown. The magnitude of the relaxation enhancement experienced by the individual back-bone amide proton has been indicated in gray scale for the corresponding side chain and its exposed surface. Right) Molecule rotated 70º clockwise about the molecular long axis.

Thioredoxin-mediated reduction of the photosystem I subunit PsaF and activation through oxidation by the interaction partner plastocyanin (Paper III)

In Paper I it was shown that the folded structure, and possibly also the functionality of luminal PsaF´ is strongly dependent on the redox state of the cysteine residues Cys8 and Cys63. As a follow-up to these results, we explored in Paper III whether the disulphide bridge between Cys8 and Cys63 is a plausible target for Trx-mediated reduction.

Recent studies by Motohasi et al. revealed a Trx-like protein called HCF164 that is active within the thylakoid lumen [52]. In these studies, HCF164 was shown to target the PSI subunit PsaN. PsaN is a fairly unexplored subunit of PSI but is considered to be a "weak" modulator of the Pc-PSI binding [53]. These results suggested to us that electron donation from Pc to PSI might be a subject of Trx-mediated regulation. To further explore this hypothesis, we decided to investigate if PsaF´ can be targeted by Trx in a similar way as PsaN [82].

Figure 15 shows the chemical-shift perturbations experienced by Pc in the presence of a fivefold excess of PsaF´, with and without DTT present (filled bars and empty bars, respectively). The significant chemical-shift changes experienced by Pc in the presence of PsaF´ belong to the back-bone amide groups of D42, E43, D44, I46, M57, E60, L62, K81, S85, K95 and V96. All these shift changes are drastically reduced when PsaF´ is thiolated by the addition of DTT. The magnitude of the chemical-shift changes upon the reduction of PsaF´ corresponds to an increase of the dissociation constant from approximately 1.4 mM to 5.3 mM for the Pc-PsaF´ complex upon reduction. The conclusion that Pc binds the thiolated form of PsaF´ with a lower affinity is also evident from the initial cross-linking experiments reported in Paper I.

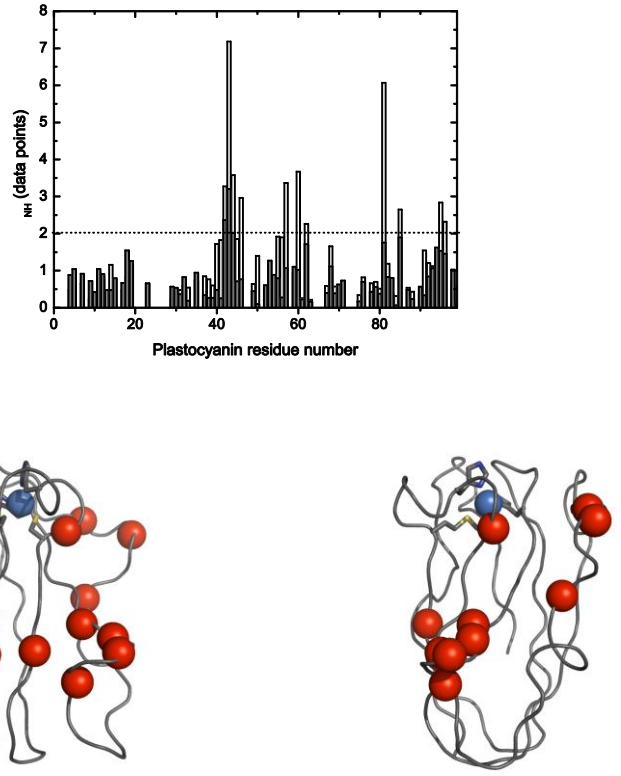

Figure 15: Upper) Show the combined chemical-shift changes of the ^{1}H-^{15}N correlation spectra experienced by ^{15}N-Pc in presence of a fivefold excess of PsaF´, with and without DTT present. Lower) Show two views of the ribbon representation of the Pc x-ray crystal structure (pdb file 1ag6) highlighting the significant chemical-shift changes indicated with black spheres. The bound copper site as well as ligands have been indicated with grey spheres and sticks, respectively.

In order to investigate whether PsaF´ is a potential target for Trx-mediated reduction and possible deactivation, we needed a method to follow the redox states of the cysteine thiols of both Trx and PsaF´. For this, we chose to use the thiol-reactive fluorophore MIANS in combination with high-resolution Tris-Tricine gel electrophoresis.

From the fluorescence electrophoresis experiments reported in Paper III, it is evident that reducing equivalents can be transferred from Trx to PsaF´, resulting in the reduction of the Cys8 and Cys63 disulphide bridge. Furthermore, it can be seen that Pc^{ox} can act as an electron acceptor in the thiol-disulphide exchange reaction. Pc^{ox} may thus facilitate the reformation of the Cys8 and Cys63 disulphide bridge in PsaF, thus, activating the domain. Figure 16 shows the time course of the reduction of Pc^{ox} in the presence of PsaF´, Trx and both PsaF´ + Trx. A faster rate of reduction can be seen when both PsaF´ and Trx are present in comparison to Trx alone. This suggests that reducing equivalents are preferentially transferred from Trx to Pc^{ox} sequentially via PsaF´.

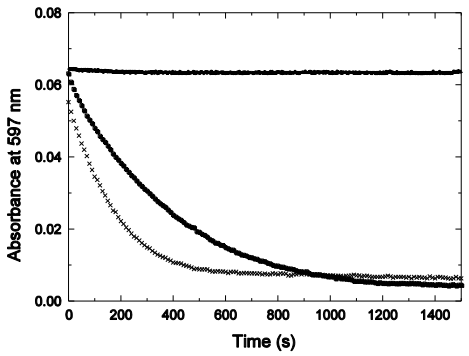

Figure 16: Time course of the absorbance at 597 nm of Pc^{ox} + PsaF´ (full line), Pc^{ox} + Trx^{red} (squares) and Pc^{ox} + PsaF ´+ Trx^{red} (crosses).

Based on these findings we propose that the electron donation to PSI is regulated *in vivo* by the redox state of PsaF. Reduction of its disulphide bridge, possibly by a Trx-like system (like HCF164), leads to a less active form to which Pc^{red} binds weakly. However, under oxidizing conditions, Pc^{ox} may reform the disulphide bridge, activating the system.

Expression of Photosystem I subunit PsaN from Arabidopsis thaliana in E. coli. (Paper IV)

The PSI subunit PsaN is located within the thylakoid lumen where it is weakly bound to the surface of PSI. Using knock-out strategies in *Arabidopsis*, Haldrup et al. have shown that the absence of PsaN, results in a reduction of the rate of electron donation from Pc to PSI with a factor of two. The effect is not as severe as for the deletion of PsaF [83]. It has been suggested that PsaN may be involved in stabilizing PsaF, indirectly facilitating a more efficient binding of Pc [53].

As mentioned in the introduction as well as in Paper III, PsaN was recently shown to be a target for thiol-disulphide exchange reactions by HCF164, a Trx-like protein found within the thylakoid lumen. Originally, the aim of our work was to over-express PsaN for characterization and interaction studies in a similar manner as we did with PsaF´ in Paper III.

A variety of different expression strategies were evaluated. Interestingly, as in the case of PsaF´, we found that PsaN was only expressed as a soluble protein when fused to Trx.

However, complications arose when trying to remove the fusion protein from PsaN. Unspecific peptide hydrolysis within the PsaN-sequence occured after the factor Xa treatment. To overcome this problem, the expression vector was modified to include a TEV-site. With this construct, a specific cleaving by TEV to remove the Trx-fusion protein from PsaN could be accomplished. The initial results were hopeful, however, as more experience were gained, degradation products appearing already after cell lysis caused serious problems when trying to isolate PsaN. This proteolytic degradation was not the same as the one observed after the Xa-treatment.

Since we were in the need of a new approach we decided to test an in-house cell-free system as an alternative to the traditional *in-vivo* based system. Positive results were obtained in the beginning for the Trx-PsaN fusion construct, showing on high levels of expression as indicated by western blots. However, two degradation products were still present as in the case of the *in-vivo* expression. Protease inhibitors are present in the cell-free system, however metal-chelating agents can not be used. This is because the *in-vitro* system relies much on a

sufficient Mg(II) content for the transcriptional and translational machinery to be functional. Hence, the cell-free system had to be abandoned.

In order to tackle the problem with proteolytical degradation of the Trx-PsaN fusion protein, we decided to evaluate the method of cell lysis, as well as additives such as EDTA and protease inhibitors. These studies showed that the proteolytical degradation of PsaN could be reduced by the presence of EDTA. Hence suggesting the involvement of a metal-dependent protease which is released upon chemical lysis.

As a result of this work, a strategy was suggested for avoiding proteolytic degradation of PsaN, a major obstacle in recombinant production of small proteins and protein domains. This work is still an ongoing project and Paper IV should be considered as a documentation of the progress made so far.

A comparative study of Cu(II) binding to angiogenin and a peptide fragment encompassing the first α-helix of the protein (paper V, related article)

My contribution to this work was to improve the purification procedures of hAng to obtain significant quantities of active protein for general characterization, functional studies and isotopical labeling for studies by NMR. A general characterization of hAng by UV-vis and stability measurements by thermofluorescence were also made by me. I developed methods for a metal-free activity assay and used it for studying the effect of Cu(II) on the ribonucleolytic activity of hAng.

The methods for solubilization and refolding of hAng from inclusion bodies were derived from the empirically optimized conditions for bovine Ang [84]. For the refolding buffer, special attention was paid to the following parameters: GSH/GSSG ratio (0.5 mM), pH (7.5-8), GdnHCL (0.3 M), NaCl (10-100 mM) and final protein concentration (0.2 mg/ml). The protein was allowed to refold for at least ~24h at 4ºC. After filtration, the sample was purified on a cation exchanger followed by SEC. The purified protein displayed a single band on SDS-PAGE and full enzymatic activity.

The improved refolding protocol resulted in approximate yields of 10 mg/L culture media. This can be compared with the original protocol for expressing hAng which results in yields of approximately 2 mg/L of culture media [85]. Furthermore, the procedure worked well for preparing ^{15}N-labeled hAng, resulting in a yield of approximately 5 mg/L minimal media.

Optical measurements in the UV-vis range were used to characterize the Cu(II) binding to hAng. As previously reported by Soncin et al., an absorption signal at 725 nm is expected for the Cu(II) bound specie of hAng [61]. However, our spectra showed an absorption band at 560 nm (ε_{560} = 120 M^{-1} cm^{-1}) already at a 1:1 hAng:Cu(II) stoichiometry, resulting in a pink color of the protein.

The Cu(II) complex formed by hAng was further characterized with EPR and CD spectroscopy and compared with data from a synthetic peptide fragment encompassing residues 4-17. The results suggest that Cu(II) is most likely bound to one of the histidines 8 or 13.

We also investigated whether the catalytic activity of hAng is affected by the presence of Cu(II). The results obtained were similar to those previously reported by Lee et al. [62]. The ribonucleolytic activity was only affected at very high levels of Cu(II), but not at a 1:1 stoichiometry. Our thermofluorescence studies indicated a significant loss in protein stability when large amounts of Zn(II) are present. This result suggests that the drop in enzymatic activity is likely related to the protein becoming unstable at higher concentrations of Cu(II).

In conclusion, at a hAng:Cu ratio of 1:1, the copper ion is most likely bound to His8, since the ribonucleolytic activity of the enzyme remains intact. This work is an ongoing collaboration with Diego La Mendola, Istituto di Biostrutture e Bioimmagini-CNR-Catania, Catania, Italy.

pH dependence of copper geometry, reduction potential, and nitrite affinity in nitrite reductase (Paper VI, related article)

My contribution to this work in consisted of anaerobic redox titrations using a glove-box system which was followed by quantitative EPR measurements of the Cu(II) Type-2 signal of

nitrite reductase. From the data analysis it can be concluded that the midpoint redox potential of the Type-2 Cu-site is pH dependent.

Acknowledgments

In the lack of time, I'm going to keep this short.

Örjan, my supervisor, it is a true challenge to find a person who knows more than you do, thank you for being a huge source of inspiration and always giving a helping hand when I need.

Jonas F., a good friend who always listen.

Martin, for always being nice and helping with the really tricky NMR-stuff.

Lars, for the great conversations and creating a nice atmosphere.

Maria, Johan, Anders, Linnéa and **Diana,** for all the great times. From Moscow, EUROMAR, to Spin-dynamics, and in to the lab again.

Bruno, Lars, Jonas C., **Lisha** and **Janne**, who made the times in the lunchroom enjoyable.

Göran and **Vladislav**, for teaching me how to work the really big magnets.

Diego, Cicco, Gaetano and **Alessio**, my Italian friends whom I hope to see more of.

Lars-Gunnar, for helping out with your biochemical expertise, it has saved us more than once.

Nicklas, for the great tips throughout the years and your feed-back.

Frida and **Richard**, for letting me in on the NiR project.

Elisabeth, for your MS expertise.

My family, for always being there, it means the world.

References

[1] H.V. Scheller, P.E. Jensen, A. Haldrup, C. Lunde, J. Knoetzel, Role of subunits in eukaryotic Photosystem I, Biochimica et Biophysica Acta (BBA) - Bioenergetics 1507 (2001) 41-60.

[2] P.E. Jensen, R. Bassi, E.J. Boekema, J.P. Dekker, S. Jansson, D. Leister, C. Robinson, H.V. Scheller, Structure, function and regulation of plant photosystem I, Biochimica et biophysica acta 1767 (2007) 335-352.

[3] A. Amunts, H. Toporik, A. Borovikova, N. Nelson, Structure Determination and Improved Model of Plant Photosystem I, Journal of Biological Chemistry 285: (2010) 3478-3486.

[4] A. Amunts, O. Drory, N. Nelson, The structure of a plant photosystem I supercomplex at 3.4 Å resolution, Nature 447 (2007) 58-63.

[5] N. Nelson, A. Ben-Shem, The complex architecture of oxygenic photosynthesis, Nat Rev Mol Cell Biol 5 (2004) 971-982.

[6] A. Ben-Shem, F. Frolow, N. Nelson, Crystal structure of plant photosystem I, Nature 426 (2003) 630-635.

[7] M. Hippler, R. Ratajczak, W. Haehnel, Identification of the Plastocyanin Binding Subunit of Photosystem-I, Febs Letters 250 (1989) 280-284.

[8] S. Jansson, B. Andersen, H.V. Scheller, Nearest-neighbor analysis of higher-plant photosystem I holocomplex, Plant physiology 112 (1996) 409-420.

[9] R.M. Wynn, R. Malkin, Interaction of plastocyanin with photosystem I: a chemical cross-linking study of the polypeptide that binds plastocyanin, Biochemistry 27 (1988) 5863-5869.

[10] P. Jordan, P. Fromme, H.T. Witt, O. Klukas, W. Saenger, N. Krauss, Three-dimensional structure of cyanobacterial photosystem I at 2.5 A resolution, Nature 411 (2001) 909-917.

[11] M. Hippler, F. Drepper, W. Haehnel, J.D. Rochaix, The N-terminal domain of PsaF: precise recognition site for binding and fast electron transfer from cytochrome c6 and plastocyanin to photosystem I of Chlamydomonas reinhardtii, Proc Natl Acad Sci U S A 95 (1998) 7339-7344.

[12] K.K. Ho, D.W. Krogmann, Electron donors to P700 in cyanobacteria and algae: An instance of unusual genetic variability, Biochimica et Biophysica Acta (BBA) - Bioenergetics 766 (1984) 310-316.

[13] B.G. Schlarb-Ridley, R.H. Nimmo, S. Purton, C.J. Howe, D.S. Bendall, Cytochrome c(6A) is a funnel for thiol oxidation in the thylakoid lumen, FEBS Lett 580 (2006) 2166-2169.

[14] F.P. Molina-Heredia, J. Wastl, J.A. Navarro, D.S. Bendall, M. Hervas, C.J. Howe, M.A. De la Rosa, Photosynthesis (communication arising): A new function for an old cytochrome?, Nature 424 (2003) 33-34.

[15] M. Weigel, C. Varotto, P. Pesaresi, G. Finazzi, F. Rappaport, F. Salamini, D. Leister, Plastocyanin Is Indispensable for Photosynthetic Electron Flow in Arabidopsis thaliana, Journal of Biological Chemistry 278 (2003) 31286-31289.

[16] L.M. Briggs, V.L. Pecoraro, L. McIntosh, Copper-induced expression, cloning, and regulatory studies of the plastocyanin gene from the cyanobacterium Synechocystis sp. PCC 6803, Plant Molecular Biology 15 (1990) 633-642.

[17] J. Mitchell Guss, H.C. Freeman, Structure of oxidized poplar plastocyanin at 1·6 Å resolution, Journal of molecular biology 169 (1983) 521-563.
[18] P.M. Colman, H.C. Freeman, J.M. Guss, M. Murata, V.A. Norris, J.A.M. Ramshaw, M.P. Venkatappa, X-ray crystal structure analysis of plastocyanin at 2.7 Ångströms resolution, Nature 272 (1978) 319-324.
[19] J.M. Moore, D.A. Case, W.J. Chazin, G.P. Gippert, T.F. Havel, R. Powls, P.E. Wright, 3-Dimensional Solution Structure of Plastocyanin from the Green-Alga Scenedesmus-Obliquus, Science 240 (1988) 314-317.
[20] M.R. Redinbo, D. Cascio, M.K. Choukair, D. Rice, S. Merchant, T.O. Yeates, The 1.5-Angstrom Crystal-Structure of Plastocyanin from the Green-Alga Chlamydomonas-Reinhardtii, Biochemistry 32 (1993) 10560-10567.
[21] Y.F. Xue, M. Ökvist, Ö. Hansson, S. Young, Crystal structure of spinach plastocyanin at 1.7 Ångström resolution, Protein Science 7 (1998) 2099-2105.
[22] D.G. Sanderson, L.B. Anderson, E.L. Gross, Determination of the redox potential and diffusion coefficient of the protein plastocyanin using optically transparent filar electrodes, Biochimica et Biophysica Acta (BBA) - Bioenergetics 852 (1986) 269-278.
[23] J.M. Guss, P.R. Harrowell, M. Murata, V.A. Norris, H.C. Freeman, Crystal structure analyses of reduced (CuI) poplar plastocyanin at six pH values, Journal of molecular biology 192 (1986) 361-387.
[24] S.R. Durell, J.K. Labanowski, E.L. Gross, Modeling of the electrostatic potential field of plastocyanin, Archives of Biochemistry and Biophysics 277 (1990) 241-254.
[25] F. Sommer, F. Drepper, W. Haehnel, M. Hippler, The hydrophobic recognition site formed by residues PsaA-Trp(651) and PsaB-Trp(627) of photosystem I in Chlamydomonas reinhardtii confers distinct selectivity for binding of plastocyanin and cytochrome c(6), Journal of Biological Chemistry 279 (2004) 20009-20017.
[26] H. Jansson, M. Ökvist, F. Jacobson, M. Ejdebäck, Ö. Hansson, L. Sjölin, The crystal structure of the spinach plastocyanin double mutant G8D/L12E gives insight into its low reactivity towards photosystem 1 and cytochrome f, Biochimica et biophysica acta 1607 (2003) 203-210.
[27] S. Young, K. Sigfridsson, K. Olesen, O. Hansson, The involvement of the two acidic patches of spinach plastocyanin in the reaction with photosystem I, Biochimica et biophysica acta 1322 (1997) 106-114.
[28] M. Hippler, J. Reichert, M. Sutter, E. Zak, L. Altschmied, U. Schroer, R.G. Herrmann, W. Haehnel, The plastocyanin binding domain of photosystem I, Embo J 15 (1996) 6374-6384.
[29] G. McLendon, Control of biological electron transport via molecular recognition and binding: The "velcro" model, Long-Range Electron Transfer in Biology, vol. 75, Springer Berlin / Heidelberg, 1991, pp. 159-174.
[30] H. Jansson, Plastocyanin - a transient link in the photosynthetic electron transfer chain, Department of Chemistry, Göteborg University, Göteborg, 2007.
[31] H. Jansson, Ö. Hansson, Competitive inhibition of electron donation to photosystem 1 by metal-substituted plastocyanin, Biochimica et Biophysica Acta (BBA) - Bioenergetics 1777 (2008) 1116-1121.
[32] D.S. Bendall, Protein Electron Transfer, 1 ed., Bios Scientific Publishers Ltd 1996.
[33] M. Prudencio, M. Ubbink, Transient complexes of redox proteins: structural and dynamic details from NMR studies, J Mol Recognit 17 (2004) 524-539.

[34] M. Ubbink, M. Ejdeback, B.G. Karlsson, D.S. Bendall, The structure of the complex of plastocyanin and cytochrome f, determined by paramagnetic NMR and restrained rigid-body molecular dynamics, Structure 6 (1998) 323-335.
[35] M. Ubbink, The courtship of proteins: Understanding the encounter complex, Febs Letters 583 (2009) 1060-1066.
[36] P.B. Crowley, M. Ubbink, Close encounters of the transient kind: protein interactions in the photosynthetic redox chain investigated by NMR spectroscopy, Acc Chem Res 36 (2003) 723-730.
[37] H. Bottin, P. Mathis, Interaction of plastocyanin with the photosystem I reaction center: A kinetic study by flash absorption spectroscopy., Biochemistry 24 (1985) 6453–6460.
[38] Pottosin, II, G. Schönknecht, Ion channel permeable for divalent and monovalent cations in native spinach thylakoid membranes, Journal of Membrane Biology 152 (1996) 223-233.
[39] A.R. Portis Jr, H.W. Heldt, Light-dependent changes of the Mg2+ concentration in the stroma in relation to the Mg2+ dependency of CO2 fixation in intact chloroplasts, Biochimica et Biophysica Acta (BBA)-Bioenergetics 449 (1976) 434-446.
[40] O. Shaul, Magnesium transport and function in plants: the tip of the iceberg, Biometals 15 (2002) 307-321.
[41] R. Ratajczak, R. Mitchell, W. Haehnel, Properties of the oxidizing site of Photosystem I, Biochimica et Biophysica Acta (BBA) - Bioenergetics 933 (1988) 306-318.
[42] K. Olesen, M. Ejdeback, M.M. Crnogorac, N.M. Kostic, Ö. Hansson, Electron transfer to photosystem 1 from spinach plastocyanin mutated in the small acidic patch: ionic strength dependence of kinetics and comparison of mechanistic models, Biochemistry 38 (1999) 16695-16705.
[43] M. Hervas, M.A. De La Rosa, G. Tollin, A comparative laser-flash absorption spectroscopy study of algal plastocyanin and cytochrome c552 photooxidation by photosystem I particles from spinach, European Journal of Biochemistry 203 (1992) 115-120.
[44] K. Sigfridsson, S. He, S. Modi, D.S. Bendall, J. Gray, Ö. Hansson, A comparative flash-photolysis study of electron transfer from pea and spinach plastocyanins to spinach Photosystem 1. A reaction involving a rate-limiting conformational change, Photosynthesis Research 50 (1996) 11-21.
[45] J.P. Jacquot, E. Gelhaye, N. Rouhier, C. Corbier, C. Didierjean, A. Aubry, Thioredoxins and related proteins in photosynthetic organisms: molecular basis for thiol dependent regulation, Biochemical pharmacology 64 (2002) 1065-1069.
[46] C.S. Sevier, C.A. Kaiser, Formation and transfer of disulphide bonds in living cells, Nature Reviews Molecular Cell Biology 3 (2002) 836-847.
[47] K. Motohashi, A. Kondoh, M.T. Stumpp, T. Hisabori, Comprehensive survey of proteins targeted by chloroplast thioredoxin, Proceedings of the National Academy of Sciences of the United States of America 98 (2001) 11224.
[48] C. Berndt, C.H. Lillig, A. Holmgren, Thioredoxins and glutaredoxins as facilitators of protein folding, Biochimica et Biophysica Acta (BBA)-Molecular Cell Research 1783 (2008) 641-650.
[49] B.B. Buchanan, Y. Balmer, Redox regulation: a broadening horizon, Plant Biology 56 (2005) 187.
[50] G. Gopalan, Z. He, Y. Balmer, P. Romano, R. Gupta, A. Héroux, B.B. Buchanan, K. Swaminathan, S. Luan, Structural analysis uncovers a role for redox in regulating

FKBP13, an immunophilin of the chloroplast thylakoid lumen, Proceedings of the National Academy of Sciences of the United States of America 101 (2004) 13945.
[51] B.B. Buchanan, S. Luan, Redox regulation in the chloroplast thylakoid lumen: a new frontier in photosynthesis research, Journal of experimental botany 56 (2005) 1439.
[52] K. Motohashi, T. Hisabori, HCF164 receives reducing equivalents from stromal thioredoxin across the thylakoid membrane and mediates reduction of target proteins in the thylakoid lumen, Journal of Biological Chemistry 281 (2006) 35039.
[53] A. Haldrup, H. Naver, H.V. Scheller, The interaction between plastocyanin and photosystem I is inefficient in transgenic Arabidopsis plants lacking the PSI-N subunit of photosystem, The Plant Journal 17 (1999) 689-698.
[54] M. Hall, A. Mata-Cabana, H.E. Åkerlund, F.J. Florencio, W.P. Schröder, M. Lindahl, T. Kieselbach, Thioredoxin targets of the plant chloroplast lumen and their implications for plastid function, PROTEOMICS 10 987-1001.
[55] J.W. Fett, D.J. Strydom, R.R. Lobb, E.M. Alderman, J.L. Bethune, J.F. Riordan, B.L. Vallee, Isolation and characterization of angiogenin, an angiogenic protein from human carcinoma cells, Biochemistry 24 (1985) 5480-5486.
[56] R. Shapiro, S. Weremowicz, J.F. Riordan, B.L. Vallee, Ribonucleolytic activity of angiogenin: essential histidine, lysine, and arginine residues, Proceedings of the National Academy of Sciences of the United States of America 84 (1987) 8783.
[57] A. Wied ocha, Following angiogenin during angiogenesis: a journey from the cell surface to the nucleolus, Archivum immunologiae et therapiae experimentalis 47 (1999) 299.
[58] J. Moroianu, J.F. Riordan, Identification of the nucleolar targeting signal of human angiogenin, Biochemical and biophysical research communications 203 (1994) 1765-1772.
[59] T.W. Hallahan, R. Shapiro, D.J. Strydom, B.L. Vallee, Importance of asparagine-61 and asparagine-109 to the angiogenic activity of human angiogenin, Biochemistry 31 (1992) 8022-8029.
[60] O. Lequin, H. Thüring, M. Robin, J.Y. Lallemand, Three Dimensional Solution Structure of Human Angiogenin Determined by 1H, 15N NMR Spectroscopy—Characterisation of Histidine Protonation States and Pka Values, European Journal of Biochemistry 250 (1997) 712-726.
[61] F. Soncin, J.D. Guitton, T. Cartwright, J. Badet, Interaction of Human Angiogenin with Copper Modulates Angiogenin Binding to Endothelial Cells* 1, Biochemical and biophysical research communications 236 (1997) 604-610.
[62] F.S. Lee, B.L. Vallee, Characterization of ribonucleolytic activity of angiogenin towards tRNA, Biochemical and biophysical research communications 161 (1989) 121-126.
[63] F.W. Studier, A.H. Rosenberg, J.J. Dunn, and, J.W. DuBendorff, Use of T7 RNA polymerase to direct expression of cloned genes, Methods in Enzymology 188 (1991).
[64] M.A. Sørensen, C.G. Kurland, S. Pedersen, Codon usage determines translation rate in Escherichia coli* 1, Journal of molecular biology 207 (1989) 365-377.
[65] J.F. Kane, Effects of rare codon clusters on high-level expression of heterologous proteins in Escherichia coli, Current Opinion in Biotechnology 6 (1995) 494-500.
[66] U. Brinkmann, R.E. Mattes, P. Buckel, High-level expression of recombinant genes in Escherichia coli is dependent on the availability of the dnaY gene product, Gene 85 (1989) 109-114.

[67] S. Gottesman, Genetics of Proteolysis in Escherichia Coli, Annual Review of Genetics 23 (1989) 163-198.
[68] P.H. Bessette, F. Åslund, J. Beckwith, G. Georgiou, Efficient folding of proteins with multiple disulfide bonds in the Escherichia coli cytoplasm, Proceedings of the National Academy of Sciences of the United States of America 96 (1999) 13703.
[69] Protein Engineering Principles and Practice, 1 ed., Wiley-Liss 1996.
[70] S. Hahn, X.Y. Zhong, C. Troeger, R. Burgemeister, K. Gloning, W. Holzgreve, Current applications of single-cell PCR, Cellular and molecular life sciences: CMLS 57 (2000) 96.
[71] R.K. Saiki, D.H. Gelfand, S. Stoffel, S.T. Scharf, R. Higuchi, G.T. Horn, K.B. Mullis, H.A. Ehrlich, Primer-directed enzymatic amplification of DNA, Science 239 (1988) 487–491.
[72] K.B. Mullis, and, F.A. Faloona, Specific synthesis of DNA *in Vitro* Via a Polymerase-Catalyzed Chain Reaction, Methods in Enzymology 155 (1987) 335-350.
[73] C. Aslanidis, P.J. De Jong, Ligation-independent cloning of PCR products (LIC-PCR), Nucleic Acids Research 18 (1990) 6069.
[74] M. Nelson, and, M. McClelland, Methods in Enzymology 216 (1992) 279-303.
[75] Principles and Techniques of Biochemistry and Molecular Biology, 6 ed., Cambridge University Press 2005.
[76] J. Porath, J.A.N. Carlsson, I. Olsson, G. Belfrage, Metal chelate affinity chromatography, a new approach to protein fractionation, Nature 258 (1975) 598-599.
[77] M.M. Crnogorac, C. Shen, S. Young, O. Hansson, N.M. Kostic, Effects of Mutations in Plastocyanin on the Kinetics of the Protein Rearrangement Gating the Electron-Transfer Reaction with Zinc Cytochrome c. Analysis of the Rearrangement Pathway†, Biochemistry 35 (1996) 16465-16474.
[78] M.Y. Ksenzenko, D.H. Kessel, B.P. Rosen, Reaction of the ArsA adenosinetriphosphatase with 2-(4'-maleimidoanilino)naphthalene-6-sulfonic acid, Biochemistry 32 (1993) 13362-13368.
[79] J.M. Hollas, Modern Spectroscopy, 3 ed., Wiley 2002.
[80] Cantor, and, Schimmel, Biophysical Chemistry Part 2, 12 ed., W. H. Freeman and Company 2001.
[81] G.S. Rule, and, K.T. Hitchens, Fundamentals of Protein NMR Spectroscopy, Springer 2006.
[82] M. Hall, A. Mata-Cabana, H.E. Åkerlund, F.J. Florencio, W.P. Schröder, M. Lindahl, T. Kieselbach, Thioredoxin targets of the plant chloroplast lumen and their implications for plastid function, PROTEOMICS 10 (2010) 987-1001.
[83] M. Hippler, F. Drepper, J. Farah, J.D. Rochaix, Fast electron transfer from cytochrome c(6) and plastocyanin to photosystem I of Chlamydomonas reinhardtii requires PsaF, Biochemistry 36 (1997) 6343-6349.
[84] S.H. Jang, D.K. Kang, S.I. Chang, H.A. Scheraga, H.C. Shin, High level production of bovine angiogenin in E. coli by an efficient refolding procedure, Biotechnology letters 26 (2005) 1501-1504.
[85] R. Shapiro, J.W. Harper, E.A. Fox, H.W. Jansen, F. Hein, E. Uhlmann, Expression of Met-(-1) angiogenin in Escherichia coli: Conversion to the authentic< Glu-1 protein* 1, Analytical Biochemistry 175 (1988) 450-461.